[2]Rodden, W. P., Giesing, J. P., and Kalman, T. P., "New Developments and Applications of the Subsonic Doublet-Lattice Method for Nonplanar Configurations," AGARD, CP-80-71, Nov. 1970 (Paper 4).

[3]Rodden, W. P., and Johnson, E. H., *MSC/NASTRAN Aeroelastic Analysis User's Guide*, The MacNeal-Schwendler Corp., Los Angeles, CA, 1994.

[4]Rodden, W. P., Taylor, P. F., and McIntosh, S. C., Jr., "Further Refinement of the Nonplanar Aspects of the Subsonic Doublet-Lattice Lifting Surface Method," International Council of the Aeronautical Sciences, Paper 96-2.8.2, Sept. 1996.

[5]Rodden, W. P., Taylor, P. F., McIntosh, S. C., Jr., and Baker, M. L., "Further Convergence Studies of the Enhanced Subsonic Doublet-Lattice Oscillatory Lifting Surface Method," *Proceedings of the International Forum on Aeroelasticity and Structural Dynamics* (Rome, Italy), Vol. III, Associazione Italiana di Aeronautica ed Astronautica, Rome, Italy, 1997, pp. 401–408.

Convergence of the Subsonic Doublet Lattice Method

Louw H. van Zyl*
Aerotek, CSIR, Pretoria 0001, South Africa

Nomenclature

C_l = lift coefficient based on wing area
h = plunge amplitude
k = reduced frequency based on wing semispan
k_r = reduced frequency based on mean wing semichord
M = Mach number
n = number of boxes in aerodynamic model
n_c = number of chordwise boxes on wing
s = wing semispan

Introduction

THE subsonic doublet lattice method[1,2] (DLM) is commonly used for the calculation of unsteady air loads on aircraft. This method can be regarded as an extension of the vortex lattice method (VLM), which is used for steady load calculation. The downwash factors in the DLM are calculated as the sum of a steady component, identical to that of the VLM, and an unsteady component. Whereas the steady component is exact, the unsteady component is approximated. Both the VLM and DLM suffer from a discretization error, the error introduced by dividing a lifting surface into finite panels. The DLM is much more sensitive to chordwise paneling than the VLM because of the oscillatory nature of the downwash of a lifting surface element in unsteady flow. In addition, the DLM suffers from an integration error, the error resulting from inaccuracies in the calculation of the unsteady component of the downwash factors. To obtain acceptably accurate results from the DLM, application guidelines must be adhered to.

Historically, the application guidelines separated the discretization and integration errors.[2,3] A minimum number of chordwise boxes per wavelength is specified to limit the discretization error, whereas a maximum box aspect ratio is specified to limit the integration error. Reference 2, which describes the use of parabolic approximations to the kernel numerators, suggests using box aspect ratios not much greater than unity and at least 25 boxes per wavelength (at the wing root). Reference 3 suggests using box aspect ratios less than three and at least 12.5 boxes per wavelength, also for a parabolic approximation.

For most aeroelastic applications, the combination of these two conditions dictate a fine spanwise paneling. Therefore, it was not necessary to address the spanwise paneling requirement explicitly. Rodden et al.[4,5] described quartic approximations to the kernel numerators and suggested that the higher degree approximation may allow the use of aspect ratios of up to 10. If such high box aspect ratios are used, attention will have to be given to convergence with respect to spanwise paneling. A minimum number of 50 chordwise boxes per wavelength (at mid-span) was suggested in Ref. 5, which is significantly more than what had previously been suggested for the parabolic approximation.

The guidelines for the number of boxes per wavelength were arrived at by refining the chordwise paneling and noting when the results became stationary to within the desired limit. The higher box aspect ratio limit suggested in Ref. 5 was arrived at by continuing the refinement of the chordwise paneling and noting that the results did not deviate from the stationary result. The discretization and integration errors were not separated in these studies. In the present study, the two sources of error are separated using a much more accurate approximation to the kernel numerators.[6]

Convergence with Respect to Chordwise Paneling

Results for a two-dimensional case are presented first to get an indication of the expected convergence behavior of the DLM in the absence of any spanwise integration error. The test case is that of an airfoil oscillating in pitch, for which Von Kármán and Sears[7] gave an analytical closed-form solution. An incompressible two-dimensional DLM was used to calculate the ratio of the unsteady moment to the steady moment at $k_r = 2$. Only the contribution of the pitching motion to the boundary condition was used, as was done in Ref. 7. Results for 16–1024 chordwise panels are plotted against $1/n$ in Fig. 1. The real and imaginary parts of the analytical result are indicated by short horizontal lines drawn onto the vertical axis. It is seen that the DLM results converge to the analytical result along approximately straight lines. The DLM results were extrapolated to an infinite number of panels ($1/n = 0$) from the last two points of each line and compared to the analytical result. The relative error, i.e., the magnitude of the difference divided by the magnitude of the analytical result, is 0.003%.

The AGARD wing and horizontal tail in plunge at $M = 0.8$ and $k_r = 1.2$ is used to illustrate the convergence behavior, with respect to chordwise paneling, of the DLM for different levels of integration error. The wing and tail are divided into eight strips at 1/6, 1/3, 1/2, 2/3, 5/6, 0.9, and 0.96 fractions of

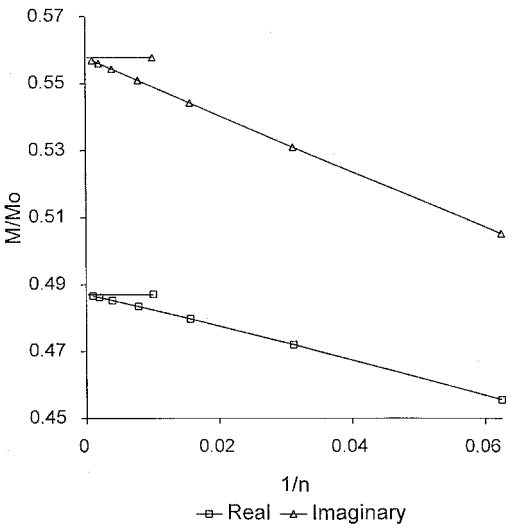

Fig. 1 Moment on an airfoil oscillating in pitch.

Received March 1, 1998; revision received July 2, 1998; accepted for publication July 8, 1998.

*Engineer, Aeroelasticity Facility, P.O. Box 395. E-mail: lvzyl@csir.co.za

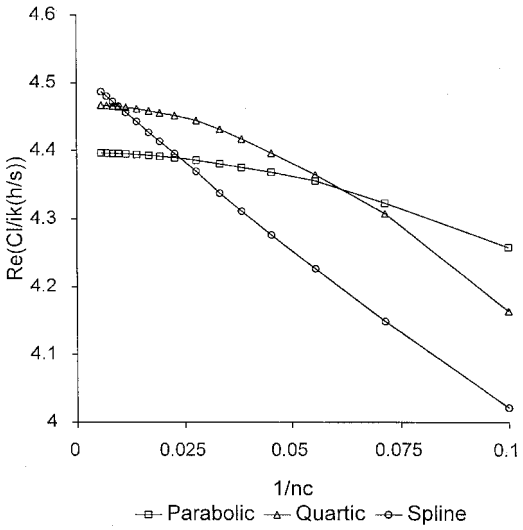

Fig. 2 Lift coefficient of AGARD wing and tail in plunge.

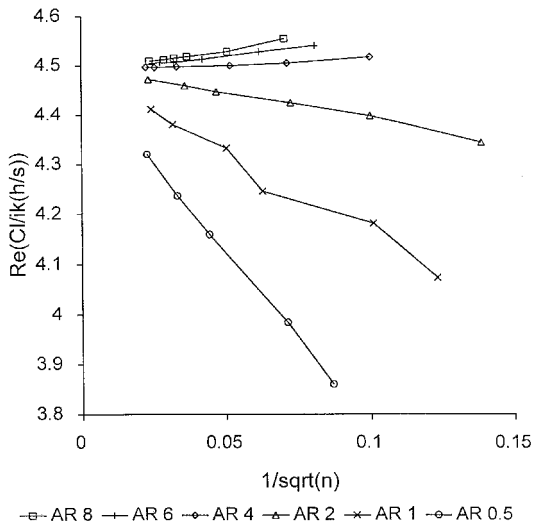

Fig. 3 Convergence histories for constant box aspect ratios.

the span, the same divisions used in Ref. 5. The wing and tail are divided into different numbers of chordwise boxes, viz., 10 and 6; 14 and 8; 18 and 10; 22 and 12; 26 and 14; 30 and 16; 36 and 20; 44 and 24; 52 and 28; 60 and 32; 72 and 40; 88 and 48; 104 and 56; 120 and 64; 144 and 80; and 176 and 96, respectively. The real parts of the normalized lift coefficient are plotted against $1/n_c$ in Fig. 2 for parabolic, quartic, and 129 point spline approximations to the kernel numerator. The results for the parabolic and quartic approximations level off for large numbers of chordwise boxes, with the results for the quartic approximation doing so at a larger number. The results for the spline approximation do not level off, but follow an approximately straight line. This is the same behavior observed for the two-dimensional case.

The results from the present implementation of the DLM using the quartic approximation to the kernel numerators match the results in Ref. 5 to the three decimal places presented there with one exception, which seems to be a reproduction error in Ref. 5: the normalized lift coefficient for 22 chordwise boxes on the wing and 12 on the tail is given as $4.396+i2.961$, whereas the present implementation calculates it as $4.396+i2.967$. The results of the present implementation using a parabolic approximation to the kernel numerator and using Laschka's 11-term exponential polynomial[8] in evaluating the kernel functions also match those presented in Ref. 5. The results for the parabolic approximation presented here were, however, calculated using Desmarais' D12.1 approximation in evaluating the kernel functions.[9]

Convergence at Constant Box Aspect Ratio

The historical guidelines do not give an indication of the fully converged solution for a particular problem, nor an estimate of the error. This can, however, easily be obtained by simultaneously refining the spanwise and chordwise paneling of a lifting surface in such a way that the box aspect ratios are kept reasonably constant. Different aerodynamic grids for the AGARD wing and tail were generated using the minimum number of boxes while satisfying restraints on maximum box aspect ratio and maximum box chord. Box aspect ratios of 8, 6, 4, 2, 1, and 0.5 were specified. A series of successively finer grids were generated for each aspect ratio by specifying a range of decreasing box chords. The aspect ratios quoted are upper limits, most boxes having smaller aspect ratios. Because of the different taper ratios of the wing and tail, it was not possible to give all boxes the same aspect ratio.

The unsteady lift coefficient of the AGARD wing and tail in plunge at $M = 0.8$ and $k_r = 1.2$ was calculated using these grids and using a quartic approximation to the kernel numerator. Figure 3 shows the convergence histories of the real part of the normalized lift coefficient. The results are plotted against $1/\sqrt{n}$, which is proportional to linear box size. The results for the different box aspect ratios converge along approximately straight lines with different slopes to practically the same value, indicating that the integration error diminishes along with the discretization error.

Conclusions

The convergence of the subsonic DLM with respect to refining chordwise paneling, as well as convergence with respect to simultaneously refining chordwise and spanwise paneling, was investigated. In the former case, this study suggests that in the absence of integration error, the DLM results would converge along approximately straight lines when plotted against box chord. The leveling off of DLM results with respect to reducing box chord is a result of the integration error introduced by the approximations to the kernel numerators and is not related to physical conditions for convergence. This explains why more chordwise boxes are required to achieve stationarity of results with respect to chordwise paneling when using the more accurate quartic approximation than when using the parabolic approximation.

In the latter case, the DLM results converge to practically the same values along approximately straight lines, regardless of the approximation to the kernel numerators used or the box aspect ratio. For practical problems the nonconvergence error can be estimated by employing two grids, one twice as fine in chordwise and spanwise paneling as the other. The difference between the results obtained from the two grids is an indication of the error in the results of the finer grid. The coarser grid must meet basic requirements to ensure reasonably linear convergence behavior. Although not illustrated here, five or more spanwise strips and four or more chordwise boxes were found to be sufficient to ensure linear convergence behavior of the DLM for rigid motions at low frequency. When applied to elastic modes of wings and wings with control surfaces, this requirement should be interpreted as five or more spanwise strips between bending mode node lines, and four or more chordwise boxes on each chordwise section (leading-edge control surface, fixed part, and trailing-edge control surface). For higher frequencies, the requirements of box size relative to wavelength may require a finer grid.

Large box aspect ratios resulting from the refinement of chordwise paneling does not have a detrimental effect on the DLM results. Rather than limiting box aspect ratio and box chord, it may be more appropriate to limit the spanwise and chordwise extent of doublet lines. This will result in a finer paneling scheme for highly swept planforms than for unswept or moderately swept planforms, which is not the case when

limiting box chord and box aspect ratio. On the other hand, it will permit paneling of delta wings with little effort and without violating the guidelines. A limit of one-quarter of a wavelength on both the spanwise and chordwise extent of a doublet line is suggested to ensure reasonably linear convergence behavior with respect to simultaneous refinement of spanwise and chordwise paneling.

References

[1]Albano, E., and Rodden, W. P., "A Doublet-Lattice Method for Calculating Lift Distributions on Oscillating Surfaces in Subsonic Flows," *AIAA Journal*, Vol. 7, No. 2, 1969, pp. 279–285.

[2]Rodden, W. P., Giesing, J. P., and Kalman, T. P., "New Developments and Applications of the Subsonic Doublet-Lattice Method for Nonplanar Configurations," AGARD, CP-80-71, Nov. 1970 (Paper 4).

[3]Rodden, W. P., and Johnson, E. H., *MSC/NASTRAN Aeroelastic Analysis User's Guide*, The MacNeal-Schwendler Corp., Los Angeles, CA, 1994.

[4]Rodden, W. P., Taylor, P. F., and McIntosh, S. C., Jr., "Further Refinement of the Nonplanar Aspects of the Subsonic Doublet-Lattice Lifting Surface Method," International Council of the Aeronautical Sciences, Paper 96-2.8.2, Sept. 1996.

[5]Rodden, W. P., Taylor, P. F., McIntosh, S. C., Jr., and Baker, M. L., "Further Convergence Studies of the Enhanced Subsonic Doublet-Lattice Oscillatory Lifting Surface Method," *Proceedings of the International Forum on Aeroelasticity and Structural Dynamics* (Rome, Italy), Vol. III, Associazione Italiana di Aeronautica ed Astronautica, Rome, Italy, 1997, pp. 401–408.

[6]Van Zyl, L. H., "Arbitrary Accuracy Integration Scheme for the Subsonic Doublet Lattice Method," *Journal of Aircraft*, Vol. 35, No. 6, pp. 975–977.

[7]Von Kármán, T., and Sears, W. R., "Airfoil Theory for Non-Uniform Motion," *Journal of the Aeronautical Sciences*, Vol. 5, No. 10, 1938, pp. 379–390.

[8]Laschka, B., "Zur Theorie der harmonisch schwingenden tragenden Fläch bei Unterschallanströmung," *Zeitschrift für Flugwissenschaften*, Vol. 11, No. 7, 1963, pp. 265–292.

[9]Desmarais, R. N., "An Accurate and Efficient Method for Evaluating the Kernel of the Integral Equation Relating Pressure to Normalwash in Unsteady Potential Flow," AIAA Paper 82-0687, May 1982.

Rapid Prediction of Wing Rock for Slender Delta-Wing Configurations

Lars E. Ericsson*
Mountain View, California 94040

Introduction

SINCE the initial experiments by Nguyen et al.[1] and Levin and Katz,[2] which showed that an 80-deg delta wing at high angles of attack exhibits the limit-cycle oscillations in roll, referred to as slender wing rock, Arena and Nelson[3,5–7] and Arena et al.[4] have been performing a series of tests and analyses of a sharp-edged 80-deg delta wing, aimed to provide insight into the fluid mechanical processes causing slender wing rock. In Fig. 1 theirexperimental wing rock results[7] are compared to those in Refs. 1 and 2. How the difference between the results in Refs. 1 and 2 was caused by the different experimental setups is discussed in Ref. 8. The likely reason that the test results in Ref. 7 show a higher maximum limit-cycle amplitude than those in Refs. 1 and 2 (Fig. 1) is that the damping provided by the bearing friction in Refs. 1 and 2 was almost completely eliminated in Ref. 7 by the use of an air bearing. The predicted start of wing rock[9] (Fig. 2) agrees well with these friction-free test results (Fig. 1). In addition to knowing when slender wing rock will start for a particular leading-edge sweep[9] (Fig. 2), the vehicle designer also needs to know how large the limit-cycle amplitude can become when the critical angle of attack is exceeded; e.g., $\alpha > 20$ deg for $\Lambda = 80$ deg (Fig. 2). A simple analysis for the determination of the maximum possible limit-cycle amplitude is described, which produces results that compare well with the experimental results in Fig. 1 for the 80-deg delta wing.

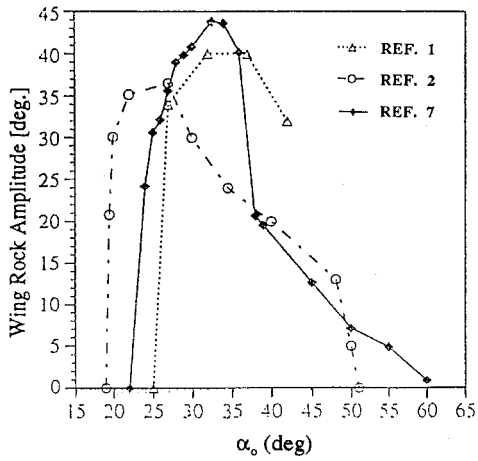

Fig. 1 Experimentally determined wing-rock-amplitude envelope for an 80-deg delta wing.

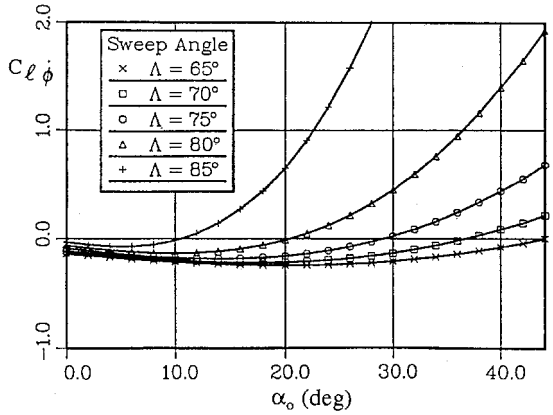

Fig. 2 Effect of leading-edge sweep on delta-wing roll damping at high angles of attack.[9]

Maximum Limit-Cycle Amplitude

Experimental results for the 80-deg delta wing[4] (Fig. 3a) show that when the roll angle is increased from $\phi = 0$ to the maximum wing rock value, $\phi = 44$ deg (Fig. 1), the left, laterally leeside vortex increases its distance above the wing surface from $\zeta_v = z_v/s \approx 0.47$ to $\zeta_v \approx 1.04$ while moving outboard from $\eta_v = y_v/s \approx -0.65$ to $\eta_v \approx -1.70$. Combining the ζ_v, η_v results in Fig. 3a gives the vortex location relative to the wing as a function of roll angle (Fig. 3b). The combined effects of the vortex-induced suction and downwash will contribute

Presented as Paper 98-0498 at the AIAA 36th Aerospace Sciences Meeting, Reno, NV, Jan. 12–15, 1998; received March 6, 1998; revision received July 10, 1998; accepted for publication July 13, 1998.

*Consulting Engineer. Fellow AIAA.